

Are your MRI contrast agents cost-effective?

Learn more about generic Gadolinium-Based Contrast Agents.



**FRESENIUS
KABI**

caring for life

AJNR

Acute disseminated encephalomyelitis: MR and CT features.

I Mader, K W Stock, T Ettlin and A Probst

AJNR Am J Neuroradiol 1996, 17 (1) 104-109

<http://www.ajnr.org/content/17/1/104>

This information is current as
of April 19, 2024.

Acute Disseminated Encephalomyelitis: MR and CT Features

I. Mader, K. W. Stock, T. Ettlin, and A. Probst

Summary: We describe three cases of acute disseminated encephalomyelitis (an immune-mediated inflammatory demyelinating disease of the central nervous system) and their histology, showing different radiological features. One appearance is a few ring-shaped enhancing lesions, which are found predominantly in the supratentorial white matter, the other is solid disseminated lesions.

Index terms: Encephalitis; Myelitis; Demyelinating disease

Acute disseminated encephalomyelitis is an uncommon immune-mediated inflammatory demyelinating disease of the central nervous system. Usually it is a monophasic illness, which may occur after viral infection, after vaccination, in association with rheumatic fever, or without any recognized antecedent disease. Radiologic findings of acute disseminated encephalomyelitis are not pathognomonic. The differential diagnosis is always difficult. Herein we describe three cases of acute disseminated encephalomyelitis and their radiologic appearance. Demyelination has been histologically verified and documented by computed tomography (CT) and magnetic resonance (MR) in each case. The combination of a clinical monophasic illness associated with histologic acute or subacute demyelination established the diagnosis of acute disseminated encephalomyelitis.

Case Reports

Case 1

Four days after returning from a journey to Kenya and 3 weeks after being vaccinated against diphtheria, tetanus, polio, and yellow fever, a 32-year-old woman presented with increasing ataxia, drowsiness, and paraesthesia in her right hand. While under clinical observation, a progressive paresis of her legs and right arm developed, as well as a

temporal lobe syndrome. Cerebrospinal fluid examination 12 days after the onset of symptoms revealed a mildly increased protein level, a normal cell count, and an absence of oligoclonal bands. During a course of steroid treatment the paresis showed a regression, and the patient was discharged. Eleven days after the onset of symptoms, cranial contrast-enhanced CT showed 11 supratentorial hypodense lesions with peripheral contrast enhancement and no perifocal edema. The lesions involved the white matter, two of them being located at the border of gray and white matter. The distribution of the lesions was strictly supratentorial (Fig 1A). Twenty-six days after the onset of symptoms and 13 days after the beginning of therapy with corticosteroids, CT showed the same lesions but no contrast enhancement. The lesions appeared more hypodense. CT showed a decrease in lesion size 17 days later. Twenty days after the onset of symptoms, 7 days after the beginning of therapy with corticosteroids, and 6 days after stereotaxic puncture, brain MR showed 11 lesions, which appeared hypointense on the T1-weighted images with only slight peripheral contrast enhancement (Fig 1B). In the proton-density images, all lesions appeared isointense compared with the surrounding brain tissue with a hyperintense halo (Fig 1C). On the T2-weighted images, the lesions were hyperintense (Fig 1D). Histologic examination showed a subacute myelinoclastic process with intact axons. Cell infiltrates consisted of numerous broad macrophages containing myelin lipid degradation products and also large hypertrophied astrocytes filling the spaces between the naked axons. A few small vessels were surrounded by thick cuffing of phagocytes mixed with lymphocytes. There were no necrotic changes of the vessel wall. The histologic changes observed were interpreted as an established early demyelinating lesion and were considered compatible with acute disseminated encephalomyelitis or multiple sclerosis. The diagnosis of acute disseminated encephalomyelitis was made because of the clinical monophasic illness.

Case 2

This 63-year-old woman presented with rapidly progressing difficulty in swallowing, a speech disorder, and a

Received May 4, 1993; accepted after revision January 18, 1994.

From the Departments of Diagnostic Radiology, Division of Neuroradiology (I.M., K.W.S.), and Neurology (T.E.), and Institute of Pathology, Division of Neuropathology (A.P.), University Hospital/Kantonsspital Basel, Switzerland.

Address reprint requests to Dr Med K. W. Stock, Department of Diagnostic Radiology, Division of Neuroradiology, University Hospital/Kantonsspital Basel, Petersgraben 4, CH-4031 Basel, Switzerland.

AJNR 17:104-109, Jan 1996 0195-6108/96/1701-0104 © American Society of Neuroradiology

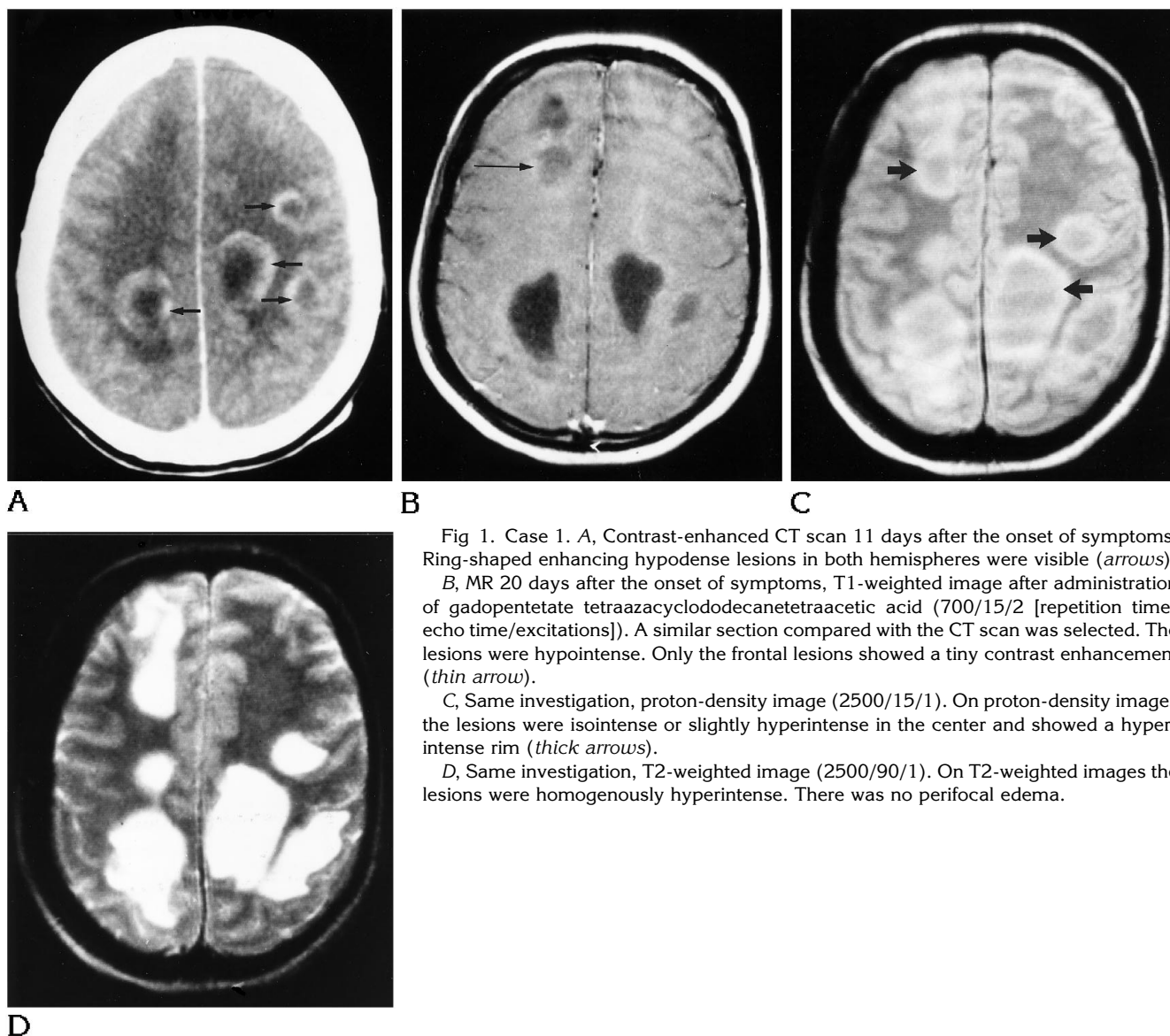


Fig 1. Case 1. A, Contrast-enhanced CT scan 11 days after the onset of symptoms. Ring-shaped enhancing hypodense lesions in both hemispheres were visible (*arrows*). B, MR 20 days after the onset of symptoms, T1-weighted image after administration of gadopentetate tetraazacyclododecanetetraacetic acid (700/15/2 [repetition time/echo time/excitations]). A similar section compared with the CT scan was selected. The lesions were hypointense. Only the frontal lesions showed a tiny contrast enhancement (*thin arrow*).

C, Same investigation, proton-density image (2500/15/1). On proton-density images the lesions were isointense or slightly hyperintense in the center and showed a hyperintense rim (*thick arrows*).

D, Same investigation, T2-weighted image (2500/90/1). On T2-weighted images the lesions were homogeneously hyperintense. There was no perifocal edema.

spastic tetraparesis. Five days after the onset of symptoms, cerebrospinal fluid examination showed a normal protein profile, a normal cell count, and an absence of oligoclonal bands. Myelin basic protein was elevated. Nine days after the onset of symptoms, cranial noncontrast and contrast-enhanced CT showed six supratentorial lesions. These were blurred and hypodense on the noncontrast scans and showed a peripheral contrast enhancement. The lesions were located in the white matter and showed no perifocal edema. One lesion was located at the border of the gray matter (Fig 2A). A biopsy was performed the next day. Fifty-two days after the onset and 48 days after the beginning of therapy with corticosteroids, CT showed seven hypodense lesions, mostly well defined, without any contrast enhancement. Brain MR 60 days after onset showed nine hyperintense lesions in the proton-density (Fig 2B) and T2-weighted images. Two lesions not seen in

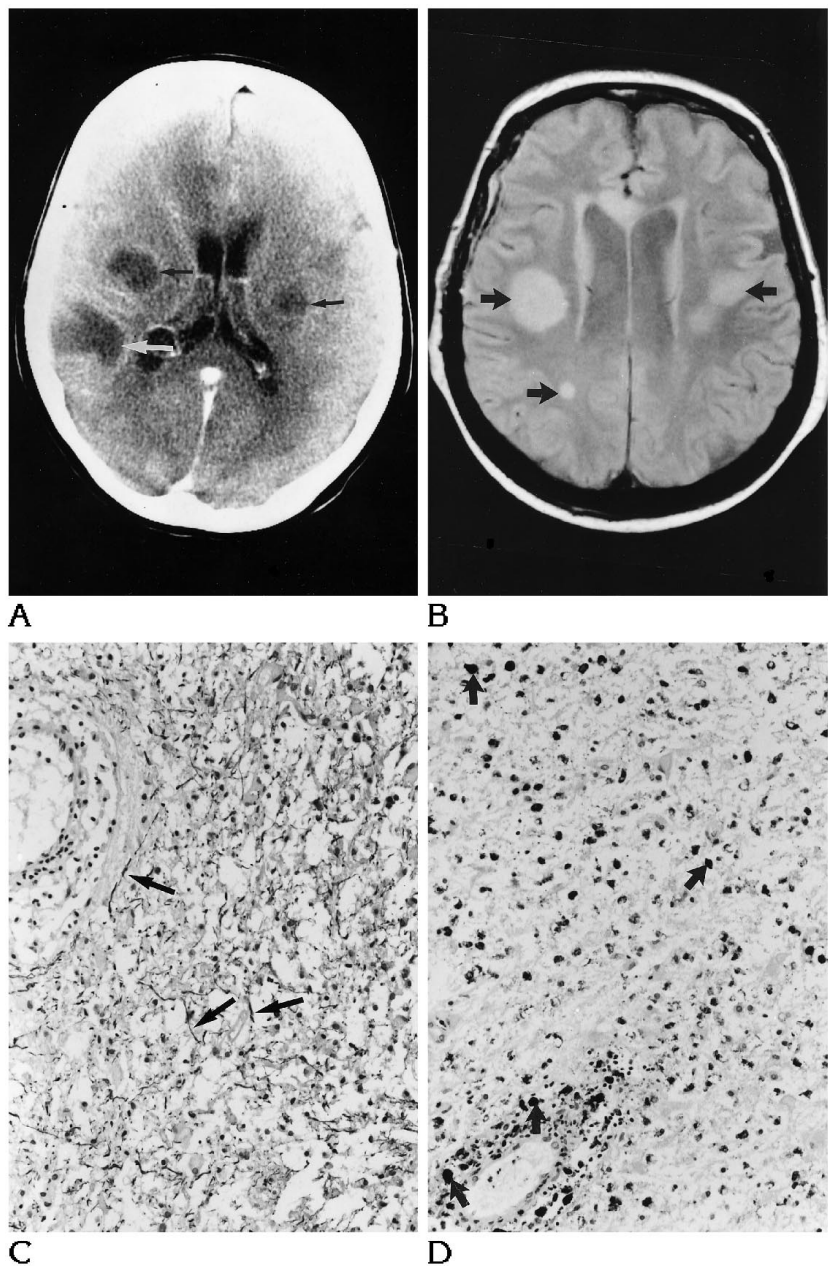
the CT scans before were located in the splenium of the corpus callosum and in the hippocampus on the right side. The postcontrast T1-weighted images showed hypointense lesions without enhancement. All lesions were seen best on the proton-density images (Fig 2B). No infratentorial lesions were found. Neurologic deficits remitted under therapy with corticosteroids. One year later, only minor neurologic deficits remained. MR 1 year later showed only seven hyperintense lesions of decreased size, which did not enhance. The main finding of histologic examination was a loosely textured and diffuse demyelinated white matter (Fig 2C). Axis cylinders within the lesions were generally preserved. Between the naked axons were large spaces filled with lipid phagocytes (Fig 2D). Some vessels within the white matter were surrounded by cuffs of tightly arranged lipid phagocytes mixed with sparse lymphocytic cells. No necrotic lesions were found in the vessel walls.

Fig 2. Case 2. A, Contrast-enhanced CT scan, 9 days after the onset of symptoms. The lesions were hypodense compared with the brain and showed a slight ring-shaped contrast enhancement (arrows).

B, MR 60 days after the onset of symptoms, proton-density image (2500/15). Unlike in case 1 these lesions, shown on proton-density images, were homogeneously hyperintense (thick arrow).

C, Loosely textured and diffusely demyelinated white matter. Numerous naked axons can be seen in the lesion as dark filiform profiles (arrows). Paraffin section immunostained with an antibody against neurofilament antigens for the demonstration of axons. Counterstain with hematoxylin (magnification, $\times 225$).

D, Same area as in C. Numerous macrophages (arrows) are seen throughout the lesion. Immunostain with monoclonal DAKO-CD68 antibodies. Paraffin section. Counterstain with hematoxylin (magnification, $\times 225$).



The ultrastructural aspect was compatible with an early demyelination. Most axis cylinders were totally devoid of myelin sheaths. Many phagocytes, some closely apposed to myelin sheaths, contained degraded myelin and lipid droplets. The light and electron microscopic aspect of the lesion was considered typical for a subacute stage of a demyelinating disease. Together with a clinical monophasic course the diagnosis of acute disseminated encephalomyelitis was made.

Case 3

This 66-year-old woman became apathetic and showed a progressive disorder of gait two weeks after a cold. On

admission 1 week later she presented with ataxia, vertigo, diplopia, and a paresis of her left leg. Furthermore, she had expressive aphasia, attention deficits, and impaired control of affect. Cerebrospinal fluid examination showed a moderate elevation of the protein level (0.6 g/L), a mononuclear pleocytosis of $9 \times 10^6/L$, and an absence of oligoclonal bands. Therapy with corticosteroids was started 1 day after biopsy and 32 days after the initial onset of symptoms. One week after the onset of initial symptoms, cranial noncontrast and contrast-enhanced CT showed 11 contrast-enhancing spots in the frontal and parietal white matter (Fig 3A). Four weeks later, CT showed seven confluent contrast-enhancing lesions located predominantly in the periventricular white matter. Twelve days after the

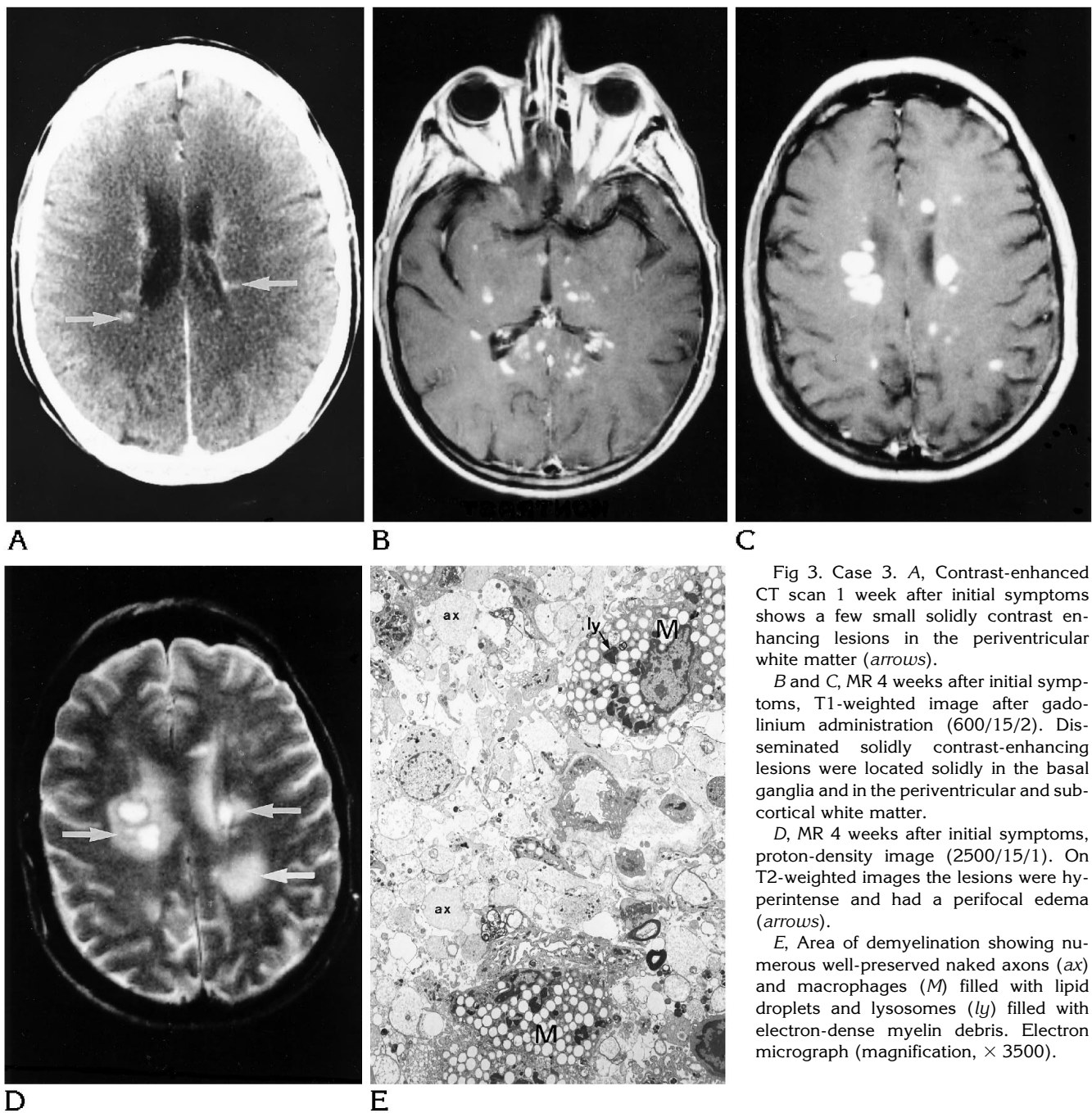


Fig 3. Case 3. A, Contrast-enhanced CT scan 1 week after initial symptoms shows a few small solidly contrast enhancing lesions in the periventricular white matter (arrows).

B and C, MR 4 weeks after initial symptoms, T1-weighted image after gadolinium administration (600/15/2). Disseminated solidly contrast-enhancing lesions were located solidly in the basal ganglia and in the periventricular and subcortical white matter.

D, MR 4 weeks after initial symptoms, proton-density image (2500/15/1). On T2-weighted images the lesions were hyperintense and had a perifocal edema (arrows).

E, Area of demyelination showing numerous well-preserved naked axons (ax) and macrophages (M) filled with lipid droplets and lysosomes (ly) filled with electron-dense myelin debris. Electron micrograph (magnification, $\times 3500$).

onset of initial symptoms, postcontrast brain MR showed 79 enhancing spots. Noncontrast T1-weighted images showed only 15 hypointense lesions. On proton-density and T2-weighted images all 79 lesions were seen as blurred hyperintense lesions with some hyperintense halo. Four weeks after the onset of symptoms, MR showed 81 enhancing lesions of increased size. Some lesions now showed a ring-shaped appearance. All lesions were hyperintense on proton-density and T2-weighted images. The perifocal hyperintensities appeared confluent (Fig 3B-D). Two months after the onset of symptoms, MR showed 40

enhancing lesions with decreased size. Some lesions were ring shaped. After 3 months MR no longer showed any enhancing lesions. Ten weeks after the initial onset of symptoms, an MR image of the cervical spine and brain stem was performed. T2- and proton density-weighted images showed five hyperintense foci in the pons, the medulla oblongata, and the upper cervical medulla without enhancement. After stereotaxic puncture of a cerebral frontal lesion, histologic examination showed an almost total demyelination in two circumscribed small areas. Axis cylinders were preserved, and infiltration by many histio-

cytic cells and large phagocytes was observed. Histiocytes and macrophages were also tightly grouped around small vessels. No necrotic changes were found in the vessel walls. Electron microscopy of the demyelination foci revealed naked axons. Some were surrounded by very thin myelin sheaths. There were many large macrophages containing lipid droplets and phagolysosomes (Fig 3E) with electron-dense myelin debris. As in cases 1 and 2, the pathologic findings were considered typical for a subacute stage of a demyelinating disease. These findings combined with the clinical monophasic illness led to the diagnosis of acute disseminated encephalomyelitis. Neurologic symptoms receded almost completely, but some expressive ataxia and affect incontinence still persist.

Discussion

The clinical and radiologic signs of the first two cases corresponded well to various descriptions of case reports of acute disseminated encephalomyelitis. The third case showed different radiologic signs. Inasmuch as there are no striking differences in the histopathology, we want to emphasize the MR appearance of acute disseminated encephalomyelitis and try to explain some of these MR features using the animal model of experimental allergic encephalomyelitis.

Pathologic findings of acute disseminated encephalomyelitis include inflammatory reactions around the vessels, edema, and perivenous demyelination (1). Vascular damage seems to be secondary to a hyperergic reaction (1). This seems to be attributable to the possible presence of viral antigens in the endothelial cells of cerebral blood vessels (2), circulating immune complex deposition, and complement activation (3). This leads to an alteration of the blood-brain barrier, which becomes visible by contrast enhancement on CT and MR (4). Increasing T1 and T2 times are also observed (5). In our cases this contrast enhancement was present only in the beginning or first period of the disease, probably attributable to the therapy with corticosteroids, which masked it in the later stages.

In our patients, the outcome of the monophasic illness, together with the histologic finding of an extensive diffuse perivenous demyelination, gave rise to the diagnosis of acute disseminated encephalomyelitis. Besides demyelination, histologic analyses in all three patients showed only slight inflammatory changes. This fact may be attributable to the subacute stage in which the biopsies were done. The subacute stages of acute disseminated encephalomyelitis

and multiple sclerosis show a similar pattern of tissue reaction, essentially characterized by macrophages filled with myelin debris and surrounding naked axons. Acute disseminated encephalomyelitis can be compared with a disease called experimental allergic encephalomyelitis (1). In experimental allergic encephalomyelitis alterations of T1 and T2 values can be detected when only prodromal symptoms are seen (5). An increase of T1 and T2 values is seen in acute lesions of experimental allergic encephalomyelitis (5). The reasons for alteration of T1 and T2 times in nonhemorrhagic lesions are not clear. They may be caused by an increase of water content, inflammation, and later astrocytosis and gliosis. Diffuse or localized contrast leakage in acute or relapsing disease points to a blood-brain barrier leakage in active stages (4) and in active demyelination (6). It is interesting that, on proton-density images in case 1, the lesions appeared ring shaped with a hypointense center and a hyperintense periphery, and that in case 2 the lesions appeared homogeneously hyperintense. The different appearance of the MR in case 1 may be attributed to its having been performed in a more acute stage of the disease. Ring-shaped enhancing lesions in case 3 never showed a ring-shaped appearance on proton-density images. Different appearances of these lesions could depend on different pathologic substrates. The central hypointense signal on proton-density images of case 1 could be explained by necrosis, the homogenous hyperintense signal in case 2 by demyelination. Histologic verification is difficult, because the amount of material obtained by puncture is very small. The persistence of the hyperintense signal in the late stage is likely to be attributable to astrocytic hyperplasia (7) or demyelination. In cases 2 and 3 the hyperintense lesions persisted after 1 year and after 5 months in proton-density and T2-weighted images, respectively. This fact supports the theory of astrocytic hyperplasia or demyelination.

On the other hand, radiologic findings and the distribution of lesions were similar in cases 1 and 2 but differed in case three. Cases 1 and 2 had almost exclusively ring-shaped enhancing lesions of roughly the same size. Case 3 had more "solid" than ring-shaped enhancing lesions. In cases 1 and 2 the lesions were preferentially located in white matter, and no infratentorial lesions were seen. These findings

correspond to previously described characteristics (3, 7, 8). Case 3 showed significantly more lesions than either cases 1 and 2, and they were smaller. The lesions were located in the infratentorial and supratentorial white matter, basal ganglia, and the spinal cord. Lesions in cerebral and cerebellar white matter and in the spinal cord are described in acute disseminated encephalomyelitis and multiple sclerosis (3, 7, 9).

In conclusion, these three cases showed variable radiologic features of acute disseminated encephalomyelitis. Cases 1 and 2 showed a few ring-shaped enhancing nearly symmetric lesions in white matter. Case 3 showed diffuse disseminated solidly enhancing lesions everywhere. Pathologic findings in all three cases have been uniform, despite the different radiologic appearances. The reasons that two cases show only a supratentorial involvement and the other shows a disseminated involvement cannot be explained by the pathologic findings or by the experimental model of the disease (experimental allergic encephalomyelitis).

References

- Poser CM. Disseminated vasculinopathy: a review of the clinical and pathologic reactions of the nervous system in hyperergic diseases. *Acta Neurol Scand* 1969;45 (suppl 37):3-44
- Poser CM. Notes on the pathogenesis of the subacute sclerosing panencephalitis. *J Neurol Sci* 1990;95:219-224
- Atlas SW, Grossmann RI, Goldberg HI, Hackney DB, Bilaniuk LT, Zimmerman RA. MR diagnosis of acute disseminated encephalomyelitis. *J Comput Assist Tomogr* 1986;10:798-801
- Hawkins DA, Munro PMG, Mackenzie F, et al. Duration and selectivity of blood-brain barrier break-down in chronic relapsing experimental encephalomyelitis studied by gadolinium-DTPA and protein markers. *Brain* 190;113:365-378
- Stewart WA, Alvord EC Jr, Hruby S, Hall LD, Paty DW. Magnetic resonance imaging of experimental allergic encephalomyelitis in primates. *Brain* 1991;114:1069-1096
- Otsuka SI, Nakatsu S, Matsumoto S, et al. Multiple sclerosis simulating brain tumor on computed tomography. *J Comput Assist Tomogr* 1989;13:674-678
- Kesselring J, Miller DH, Robb SA, et al. Acute disseminated encephalomyelitis MRI findings and the distinction from multiple sclerosis. *Brain* 1990;113:291-302
- Van der Meyden CH, de Villiers JFK, Middlecote BD, Terblanché J. Gadolinium ring enhancement and mass effect in acute disseminated encephalomyelitis. *Neuroradiology* 1994;36:221-223
- Caldemeyer KS, Smith RR, Harris TM, Edwards MK. MRI in acute disseminated encephalomyelitis. *Neuroradiology* 1994;36:216-220